Machining Science and Technology, 10:197–218

ISSN: 1091-0344 print/1532-2483 online
DOI: 10.1080/10910340600710105

Taylor & Francis
Taylor & Francis Group

IMPROVING FATIGUE STRENGTH OF METALS USING ABRASIVE WATERJET PEENING

D. Arola, A. E. Alade, and W. Weber □ *Department of Mechanical Engineering, University of Maryland Baltimore County, Baltimore, Maryland, USA*

□ *Abrasive waterjet (AWJ) peening has been proposed as a viable method of surface treatment for metal orthopedic devices. In this study the influence of AWJ peening on the compressive residual stress, surface texture and fatigue strength of a stainless steel (AISI 304) and titanium (Ti6Al4V) alloy were studied. A design of experiments (DOE) and an analysis of variance (ANOVA) were used to identify the primary parameters contributing to the surface texture and magnitude of surface residual stress. The influence of AWJ peening on the fatigue strength of the metals was evaluated under fully reversed cyclic loading. It was found that AWJ peening results in compressive residual stress and is primarily influenced by the abrasive size and treatment pressure. The residual stress of the AISI 304 ranged from 165 to over 460 MPa. Using the optimum treatment parameters for maximizing the residual stress, the endurance strength of Ti6Al4V was increased by 25% to 845 MPa. According to results of this study AWJ peening is a viable method of surface treatment for applications that require an increase in surface roughness and maintenance or increase in fatigue strength, qualities that most often are not available from a single process.*

Keywords Abrasive Waterjet, Fatigue, Implant, Surface Treatment

INTRODUCTION

Fatigue is an important concern in the design of engineering components. History has shown that fatigue failures generally originate at the surface of components. Service induced flaws, environmental factors, and the surface texture/surface integrity resulting from manufacturing processes are all sources for premature failure. Fatigue failures are also a critical concern in the field of orthopedics, and especially in the design of load bearing metal implants (1).

The requirements placed on the surface of metal implants are slightly different than those for standard machine elements. The surface texture of implants, particularly those of the hip and knee, must support fixation of

Address correspondence to D. Arola, Department of Mechanical Engineering, University of Maryland Baltimore County, 1000 Hilltop Circle, Baltimore, MD 21250 USA. E-mail: darola@umbc.edu

the device while simultaneously maintaining high fatigue strength. Fixation is achieved through mechanical interlock between the device and bone (from direct ingrowth of bone on the device) or between the device and bone cement (for situations requiring a grouting material for placement and load transfer). Porous coatings have been applied to the surface of metal prosthetic devices to promote mechanical interlock and even to invoke surface chemistry to stimulate bone growth through an increase in osteoconductivity (2). Three of the most common methods/coatings used for metal implants include sintering of metal beads, diffusion bonding of a wire mesh and deposition of metallic plasma sprays. Clinical reports have substantiated the benefits of these surfaces to the long-term success of implanted components (3–6). According to intermediate post-surgery follow-ups (5-6 years), porous coated components have the ability to maintain fixation with probability of survival exceeding 0.95 (7, 8).

While porous coatings are considered essential for stable primary fixation, the fatigue strength of porous coated devices is often less that that of the metal in wrought form (1, 9–13). The reduction in fatigue strength is attributed to stress concentrations posed by the porous surface topography and through microstructural changes that result from deposition. Early component failures (1 to 3 years post-operative) are nearly always associated with fatigue crack initiation at the textured surface (14, 15). Residual stresses resulting from thermal treatments (16–18) are another important aspect of the surface integrity of orthopedic implants. Compressive residual stresses are effective at increasing the apparent fatigue strength and as such, surface treatments are often employed preceding plasma spray treatments (e.g., grit blasting and shot peening) (19, 20). Nevertheless, it would be far more advantageous if a single process could provide the desired surface texture, surface chemistry and residual stress distribution simultaneously.

Abrasive waterjet (AWJ) peening is a newly developed method of surface treatment that has been proposed for orthopedic applications. The process utilizes a high pressure waterjet laden with particles of specific hardness and chemistry. Recent studies on AWJ peening of metals have shown that the process is capable of introducing a surface texture that supports mechanical interlock, results in compressive residual stress, and that particles can be impregnated within the substrate to provide the desired surface chemistry (21–23). While promising, the influence of the surface texture and residual stress resulting from AWJ peening on the fatigue strength of the substrate remains unknown. The overall objective of this study was to identify the influence of AWJ peening of orthopedic metals on residual stress and fatigue strength. The specific goals were to identify the optimum parameters for maximizing the compressive residual stresses and to perform a fatigue life evaluation of metals treated using the optimum process parameters.

MATERIALS AND METHODS

Stainless steel (AISI 304) and a titanium alloy (Ti6Al4V) were utilized, as they are both representative orthopedic metals. The stainless steel has an elastic modulus of 193 GPa, density of 8000 Kg/m^3, and yield and ultimate tensile strength of 318 and 770 MPa, respectively. Similarly, the Ti6Al4V has an elastic modulus of 114 GPa, density of 4420 Kg/m^3, and yield and ultimate tensile strength of 1114 MPa and 1220 MPa, respectively. The metals were obtained in wrought form as sheet with thickness of 1.52 mm and as rod with diameter of 12.7 mm. Rectangular specimens were prepared from the sheet of AISI 304 with dimensions of 18 mm × 127 mm for an evaluation of surface texture and residual stress resulting from AWJ peening. Cylindrical fatigue specimens were prepared from the round stock of both metals according to the standard RR Moore configuration for fatigue tests with 12.7 mm grip section and 6.35 mm gage section.

An OMAX Model 2652 abrasive waterjet was used for the surface treatments. The nozzle assembly consisted of a 0.36 mm diameter sapphire orifice and a tungsten carbide mixing tube of 0.9 mm internal diameter and 89 mm length. In all treatments the nozzle was oriented perpendicular to the target surface (Figure 1a). The beam specimens were held rigidly in an aluminum fixture and treatments were conducted according to the pattern in Figure 1(b) to insure that complete coverage was achieved. Treatment of the AISI 304 rectangular beams was conducted according to a 9-run, 3-level, 4-factor Design of Experiments (DOE) (24, 25). The parameters involved in the DOE were selected according to results of previous studies (22, 23) and included the standoff distance, jet pressure, traverse speed and the abrasive size. Surface treatments for orthopedic applications may employ aluminum oxide particles or other biocompatible ceramic formulation (e.g., hydroxyapatite). Yet, garnet was used in the present study based on its availability and low cost. A particle flow rate of 0.3 kg/min was used for all treatments, regardless of the particle size. Each of the 4 selected parameters was utilized at three different levels as indicated in Table 1. Three separate 9-run arrays were implemented to achieve a fully crossed DOE and were identified as the "low," "medium" and "high" level arrays. Parametric conditions for the low level array are shown in Table 2 and conditions for the medium and high level arrays are simple permutations of the low level array (24, 25). A total of 27 unique surface treatments were performed with the AISI 304 according to the DOE.

Surface profiles of the treated specimens and the corresponding surface roughness parameters were obtained using a commercial contact profilometer (Hommel T8000 stylus surface, Hommel America). The profiles were obtained using a skidless contact probe with 10 μm diameter, traverse length of 4.8 mm, and cutoff length of 0.8 mm. Three profiles were obtained

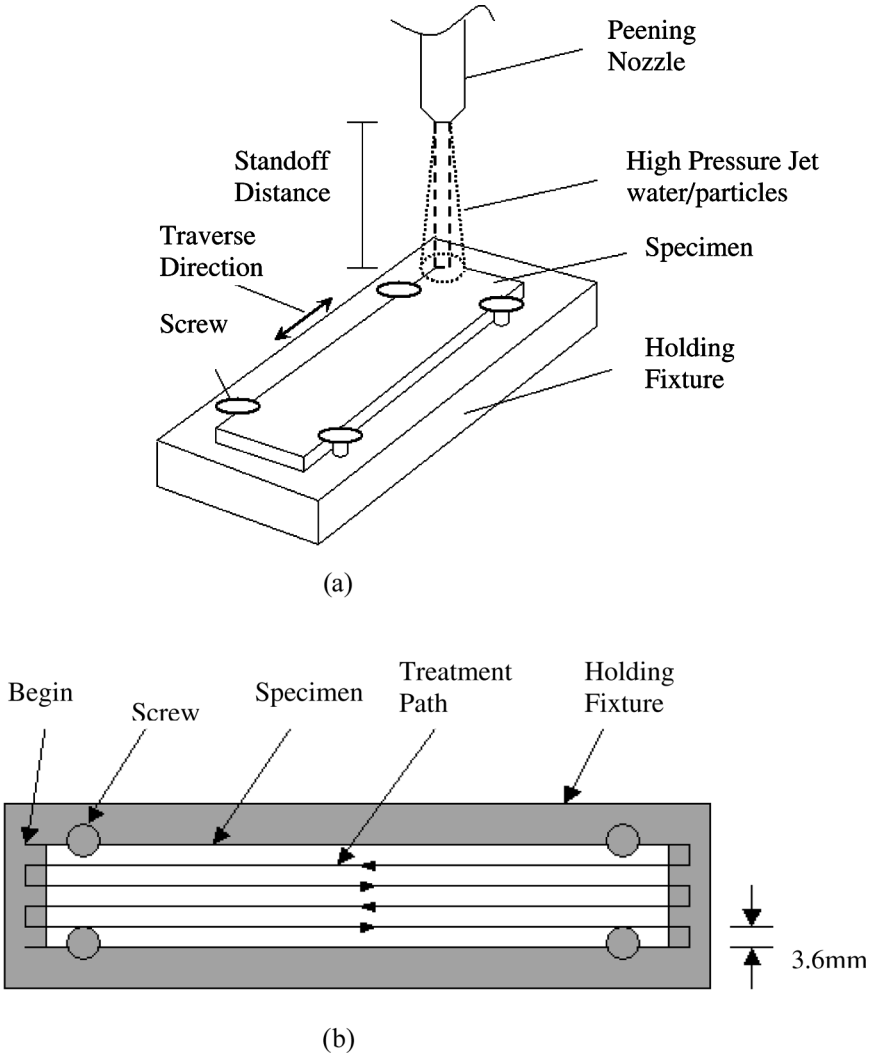

FIGURE 1 Details of the AWJ treatments. (a) Nozzle orientation and process of conducting AWJ peening of the flat metal targets. (b) Fixture and treatment path.

TABLE 1 The Surface Treatment Parameters and Levels Used for AWJ Peening

	Parameters			
Level	Standoff (S) (mm)	Pressure (P) (MPa)	Traverse (T) (m/min)	Particle size (G) (Mesh #)
Low	152	103	1.02	120
Medium	203	172	1.52	80
High	254	262	2.03	54

TABLE 2 Low-Level 9-Run Design of Experiments and Typical Treatment Responses

	Parameters				Responses	
Run 1	Standoff (mm)	Pressure (MPa)	Traverse (m/min)	Particle size (Mesh #)	Avg. Surface Roughness R_a (μm)	Residual Stress σ_r (MPa)
1	152	103	1.02	120	7.54	203
2	152	172	1.52	80	8.37	272
3	152	262	2.03	54	13.64	438
4	203	262	1.02	80	10.42	461
5	203	103	1.52	54	7.07	247
6	203	172	2.03	120	5.07	192
7	254	172	1.02	54	8.84	424
8	254	262	1.52	120	6.86	228
9	254	103	2.03	80	5.88	228

The Medium and High-Level 9-Run Designs are simple permutations on this Low-level array.

parallel to the traverse direction (of treatment) at three different locations. The average surface roughness (R_a) and core roughness parameters (R_k, R_{pk}, and R_{vk}) were obtained from the average of the three profiles. Prior to the AWJ surface treatments all specimens had an initial R_a less than 1 μm. Residual stress in the surface of the beams was determined according to the curvature resulting from elastic recovery (Figure 2a). The arc height or deflection (x) resulting from elastic recovery and the deflected beam chord length (y) was measured using dial calipers (Figure 2b). The curved beams were assumed to have a constant radius of curvature over the entire length due to uniform surface treatment. Thus, the radius of curvature (ρ) was estimated according to

$$\rho = \mathrm{x}^2 + \left(\frac{\mathrm{y}}{2}\right)^2 \cdot \frac{1}{2\mathrm{x}} \tag{1}$$

where x and y are obtained directly from experimental measurements. The beam curvature was treated as if it resulted from a uniform moment distributed over the length of the beam. Using the moment relation for beam curvature, the longitudinal residual stress (σ_r) at the surface of the beam is given by

$$\sigma_r = E \cdot \frac{t}{2} \cdot \frac{1}{\rho} \tag{2}$$

where E is the elastic modulus and t is the beam thickness. Note that the evaluation simplifies the residual stress by approximating the stress at the surface of the beam according to a linear distribution resulting from a moment equivalent in magnitude to that evident from the curvature. While

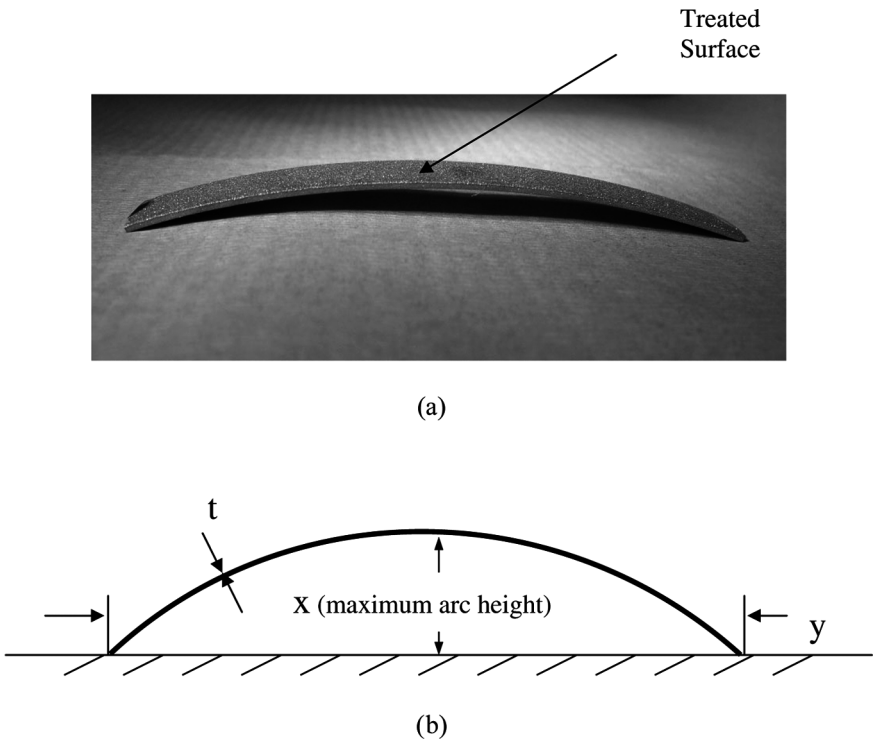

FIGURE 2 Estimation of residual stress within the AWJ peened sheet material from the curvature. (a) Oblique view of an AWJ peened beam specimen. (b) Schematic diagram of the beam deflection and experimental measures.

the method provides a useful means for comparing residual stress over the range of treatment parameters it does not provide the subsurface distribution available from the layer removal method (26). All of the rectangular AISI 304 beams were obtained from a flat sheet with no apparent curvature. Thus, the initial deflection of the specimens was small and ignored in the residual stress analysis. A preliminary analysis of residual stresses resulting from this approach was performed to assess repeatability in the AWJ peening process and potential errors introduced by the deflection measurements. It was found the variation in residual stress attributed to deflection measurements and due to process variation was ± 5 MPa. Over the total range in residual stress these factors constituted less than 3% variation.

An Analysis of Variance (ANOVA) was conducted with the surface roughness and residual stress measurements to identify the treatment parameters contributing to the dependent variables. Single parameter linear, quadratic, and two parameter interaction effects were considered in the ANOVA. Nonlinear regression models were developed for the dependent variables in terms of the treatment parameters using a commercial statistical package

(Statistical Analysis Software (SAS) Version 9.0). A second order polynomial was developed for the average surface roughness and residual stress in terms of the independent variables. An average of the relative contribution was obtained for the three 9-run arrays, and parameters with insignificant effects ($\leq$3%) were excluded from the empirical model. Empirical models were developed to obtain a quantitative understanding of the influence from treatment parameters on the dependent variables (surface texture, residual stress) over the entire treatment space. The models were also used in obtaining the optimum treatment conditions for maximizing fatigue life, i.e., the largest residual stress and lowest surface roughness.

Treatment conditions that yielded the maximum and minimum residual stress in the AISI 304 sheet were identified from the regression model and used in treatment of fatigue specimens of both AISI 304 and Ti6Al4V. Residual stresses resulting of AWJ peening of the Ti6Al4V sheet were not evaluated based on economic constraints. Though the residual stress resulting from treatment of the AISI 304 and Ti6Al4V with the same conditions are not expected to be the same, conditions resulting in the highest and lowest residual stress were assumed equivalent for both metals. A minimum of 20 specimens was treated with each unique set of parametric conditions chosen for investigation. The beams were rotated during treatment at 1000 rev/min using a dedicated frame and pneumatic motor. The machine was placed within the working envelope of the AWJ and the specimens were rigidly held between two collets (Figure 3). Due to

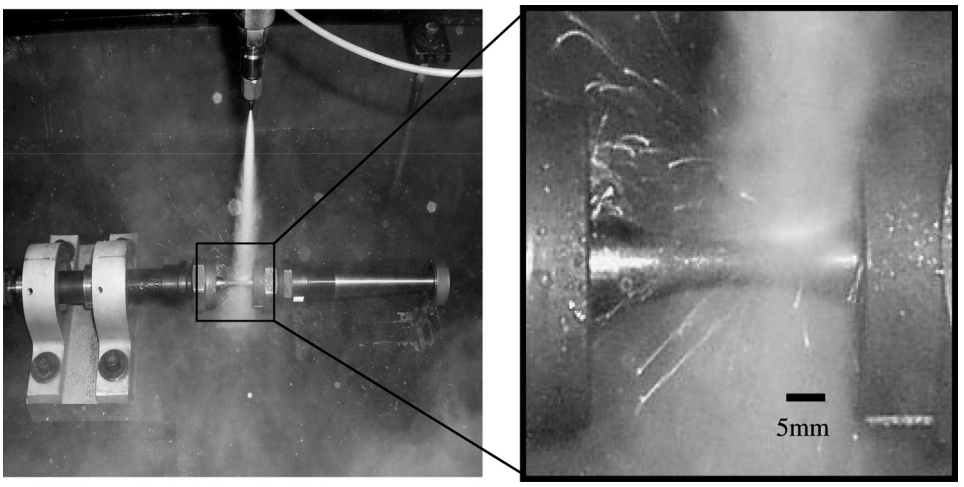

FIGURE 3 AWJ peening of the fatigue specimens. (a) Overview of treatment. (b) Specimen between the collets.

rotation of fatigue specimens during the treatments it was necessary to determine the traverse rate that resulted in an equivalent treatment intensity as that used in treatment of the beams; treatment intensity is defined as the treatment time per unit area of coverage. An additional set of surface treatments was conducted to identify the treatment intensity that resulted in saturation of the residual stress. Ten flat beams (Figure 1) of AISI 304 were prepared and treated with the treatment conditions that resulted in the maximum residual stress, except for the traverse rate, which was varied to obtain intensities from 0.01 to 0.05 $\mathrm{sec/mm^2}$. In treatment of AISI 304, the surface roughness of flat beam and cylindrical fatigue specimens were compared to insure consistency. However, residual stresses in the fatigue specimens could not be estimated according to Equation 2 due to the cylindrical geometry and axysymmetric treatment. Future experiments are planned in which the residual stresses will be analyzed using X-ray diffraction. Fatigue specimens of Ti6Al4V were treated using the optimum conditions from results of the AISI 304. While the residual stress within the AISI 304 and Ti6Al4V resulting from AWJ peening are not expected to be the same, the conditions resulting in maximum residual stress were assumed to be the same. Thus, both the AISI 304 and Ti6Al4V fatigue specimens were treated using the same conditions.

Fatigue testing of the AISI 304 and Ti6Al4V specimens was conducted at room temperature under fully reversed fatigue ($R = -1$) using a standard R.R. Moore rotating bending machine (Model RBF 200; Fatigue Dynamics, Inc. Walled Lake, MI). The fatigue tests were initiated using a bending moment that resulted in a maximum bending stress near 65% of the ultimate tensile strength of the material. The staircase method was implemented for fatigue testing (27). All the AISI 304 specimens were cycled to failure or 1.2×10^6 cycles, depending on whichever occurred first. According to the staircase method, the maximum bending stress used for successive specimens was either increased or decreased depending on whether or not failure occurred below 10^6 cycles. Specimens without treatment served as the control and were also tested using the same approach to obtain the fatigue life distribution. The stress life responses of the AWJ peened and control (unpeened) specimens were obtained by plotting the number of cycles to failure in terms of the maximum bending stress. The fatigue life distribution of the specimens was modeled according to a power law distribution in the form

$$\sigma = AN_f^b \tag{3}$$

where A and b are the stress life coefficient and exponent, respectively. Results of the model were used in estimating the apparent endurance

strength of the metals and changes in fatigue strength resulting from the AWJ surface treatment. Fracture surfaces of the specimens were examined using a Nikon SMZ 800 stereomicroscope and JEOL Model 5600 scanning electron microscope (SEM) to identify additional features characterizing the source of failure.

RESULTS

The average surface roughness resulting from AWJ peening of the AISI 304 beams ranged from 5 to nearly 14 μm. Specific results for specimens of the low level 9-run array are listed in Table 2. In general, the treatments with large abrasives and high jet pressure resulted in the highest surface roughness. Results from the ANOVA for the R_a are presented in terms of a scree plot in Figure 4. A partition line was introduced at the transition between main effects and secondary effects. Treatment effects that fall above the partition line are influential to the R_a and are regarded as responses while those falling below the partition line are regarded as rubble (minimal effect). The transition between influential and non-influential factors is identified from the change in slope of the scree plot. Note that the jet pressure (P) and particle size (G) were the most influential parameters to the surface texture and were the only two linear main effects. The standoff distance contributed to variation in R_a through interaction effects. Considering linear and quadratic effects of single treatment parameters, the particle size and jet pressure, combined for nearly 50% of the total variation in surface texture. Results of the ANOVA for R_a were

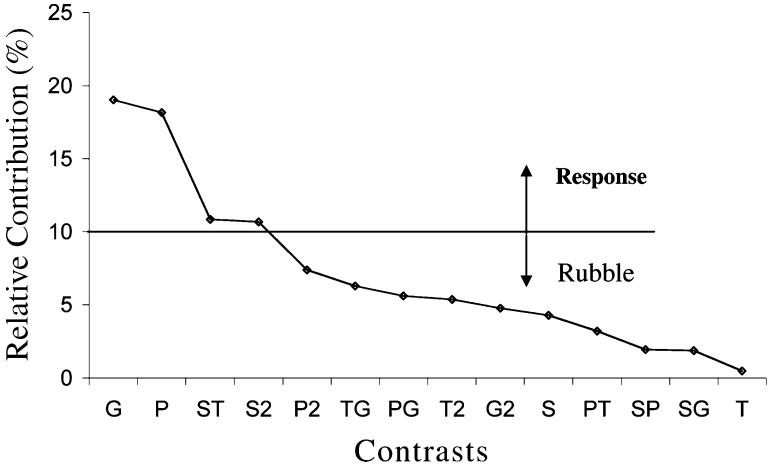

FIGURE 4 Scree plot showing relative contributions of treatment effects on the total variation of surface roughness (R_a).

consistent with the effects on R_k and R_{vk}. An empirical model was developed for the R_a and is given by

$$\begin{aligned} R_a(\mu\text{m}) = 7.80 &- (3.65E^{-2}G) + (3.0E^{-2}P) + (5.0E^{-4}G^2) \\ &- (2.05E^{-5}S^2) + (1.0E^{-4}P^2) - (2.86E^{-1}T^2) \\ &+ (1.9E^{-5}S * T) + (2.9E^{-3}T * G) - (6.0E^{-4}P * G) \end{aligned} \quad (4)$$

where G, P, S and T correspond to the particle size, jet pressure, standoff distance and traverse speed, respectively. A correlation coefficient of 0.94 was obtained in development of the model. In a comparison of the average surface roughness (R_a) predicted using Equation 4 with experimental results (over all parametric conditions of the DOE) the maximum error was 16% and the average error was less than 4%. Using Equation 4 the influence of jet pressure and grit size on the R_a is presented in Figure 5; the standoff distance and traverse rate used for this plot were 0.2 m and 1.52 m/min, respectively. As evident in this figure the R_a increased with increasing jet pressure and particle size and the largest R_a occurred with the maximum pressure (262 MPa) and abrasive size (mesh #54). A further increase in R_a appears to be possible through use of larger particles and jet pressure than those used in the present study.

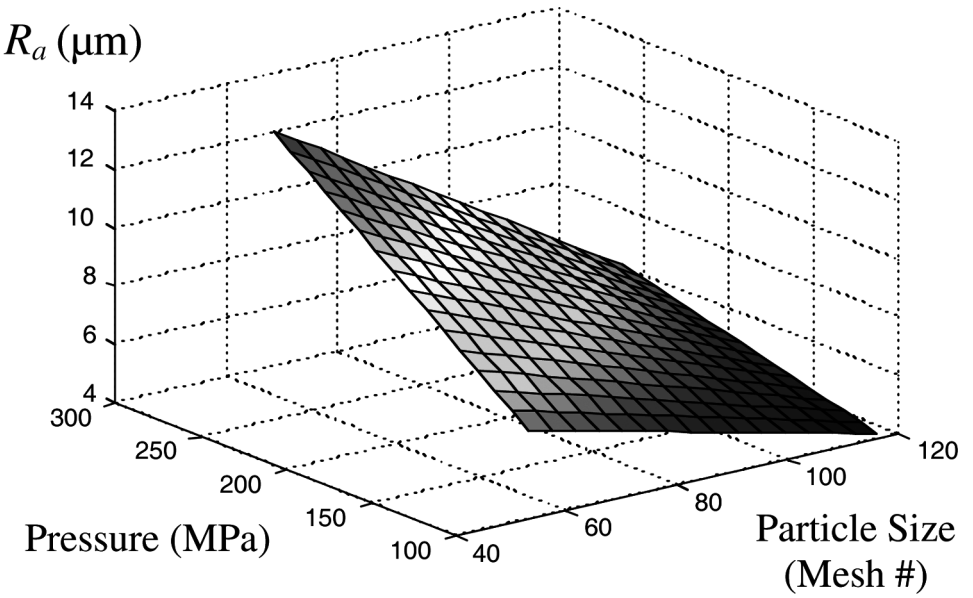

FIGURE 5 The influence of jet pressure and grit size on the average surface roughness. The contour plot was developed using a standoff distance and traverse rate of 0.2 m and 1.52 m/min, respectively.

Following AWJ peening all specimens exhibited concave deflection away from the treated surface indicating the development of compressive residual stresses (Figure 2a). There was a large range in curvature of the treated specimens that appeared to be related to the treatment parameters. Residual stress was estimated from the deflection and corresponding curvature according to Equations 1 and 2. Results for the AISI 304 specimens treated with the conditions of the low level 9–run arrays are listed in Table 2. Over the entire 27-run DOE the deflection (x: Figure 2b) ranged from 4 to 12 mm and the compressive residual stress ranged from 165 MPa to 463 MPa. In general, the specimens with large residual stresses were treated with either the largest size abrasives or highest jet pressure. The specimen with highest residual stress was treated with jet pressure of 262 MPa, #80 mesh abrasive, traverse rate of 1.02 m/min and standoff distance of 0.25 m. Conditions resulting in the lowest residual stress consisted of jet pressure of 172 MPa, #120 mesh abrasive, traverse rate of 2.03 m/min and standoff distance of 0.25 m. Results of the ANOVA performed with the residual stress measurements are presented in Figure 6. Consistent with the parametric effects on surface roughness the jet pressure and particle size were the two most influential parameters to residual stress. Considering linear and quadratic effects, the particle size (G) and jet pressure (P) accounted for more than 25% and 15% of the total variation in residual stress, respectively. According to results of the ANOVA, the magnitude of compressive residual stress increased linearly with an increase in jet pressure and particle size. A non-linear regression model was developed to

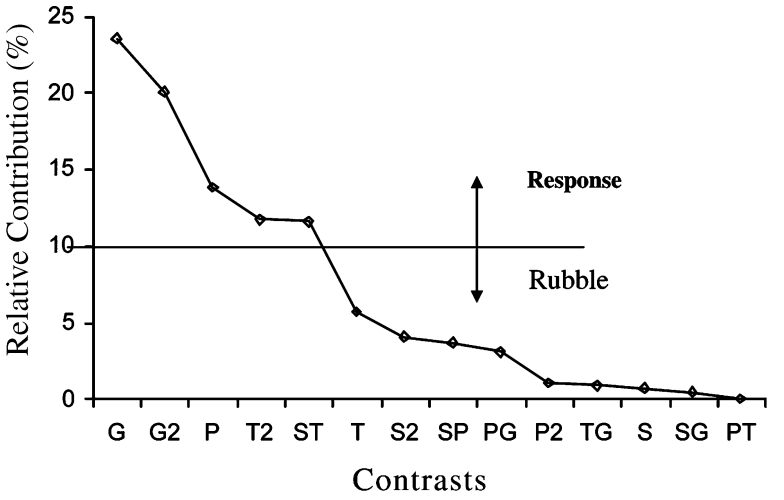

FIGURE 6 Scree plot showing relative contributions of treatment effects on the total variation of residual stress.

describe the residual stress resulting from AWJ peening and is given by

$$\begin{aligned}\sigma_r(\text{MPa}) = 138.85 &+ (3.37G) + (1.47P) + (33.46T) + (2.2E^{-3}S) \\ &- (1.86E^{-2}G^2) + (44.04T^2) - (7.99E^{-1}S * T) \\ &+ (2.8E^{-3}S * P) - (1.56E^{-2}P * G) \end{aligned} \quad (5)$$

A correlation coefficient of 0.94 was obtained. In a comparison of the residual stress estimated according to Equation 5 with experimental results from the 27 runs of the DOE, the maximum error was approximately 17% and the average error was less than 5%. Using the empirical relation for residual stress (Equation 5) the influence of these two parameters on residual stress is presented as a contour plot in Figure 7. The largest residual stress over the treatment space was approximately 460 MPa and resulted from treatment with the highest pressure and largest abrasive size (smallest mesh #). Larger compressive residual stresses may be possible with use of larger treatment pressures and particle sizes than those used in the present study. However, an increase in both pressure and grit size may eventually facilitate material removal, which may result in a reduction of residual stress through stress relief. This statement is also dependent on the relative erosion resistance of the material.

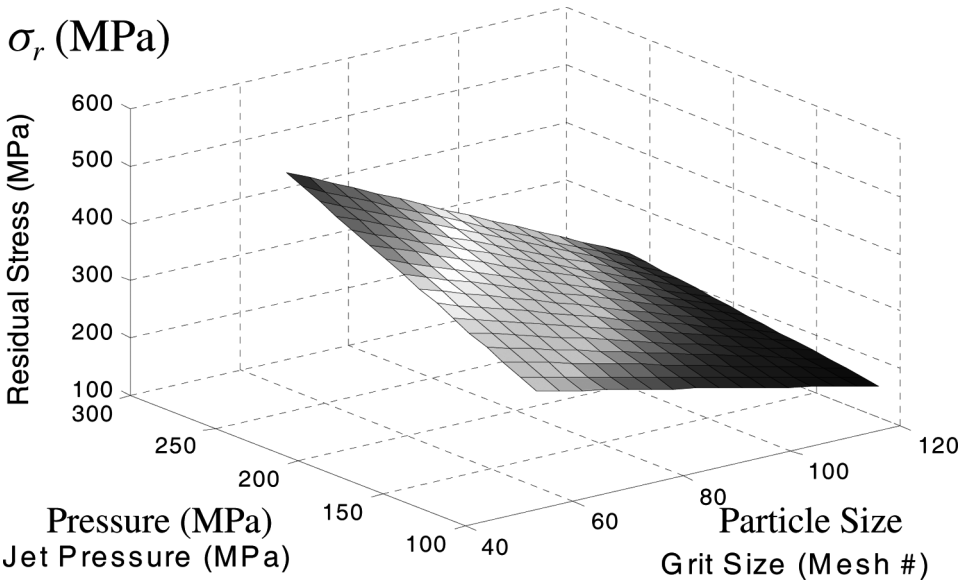

FIGURE 7 The influence of jet pressure and grit size on the average residual stress. The contour plot was developed using a standoff distance and traverse rate of 0.2 m and 1.52 m/min, respectively.

The influence of AWJ peening on the fatigue strength of AISI 304 was studied using the treatment conditions that resulted in the smallest and largest residual stress over all conditions of the DOE and are referred to here as AWJ A and AWJ B. Although the residual stress within the fatigue specimens was not measured, it was assumed that conditions resulting in the largest residual stress in the AWJ peened beams also resulted in the largest residual stress in the fatigue specimens. The R_a and core roughness parameters (R_k, R_{pk}, and R_{vk}) of the fatigue specimens were within 5% of those from the AWJ peened beam specimens treated with the same conditions. Abrasive waterjet peening of the AISI 304 stainless steel resulted in an increase in fatigue strength over the entire stress-life response (Figure 8a). Specimens with highest residual stress and surface roughness (AWJ B) yielded the largest increase in fatigue strength. According to Equation 3 the apparent endurance strength of the untreated AISI 304 specimens (at 1×10^6 cycles) was 342 MPa. AWJ peening of the specimens with condition AWJ A increased the endurance strength to 370 MPa. Treatment AWJ B resulted in apparent endurance strength of 382 MPa, which corresponds to an increase of approximately 10%. An evaluation of fatigue strength resulting from AWJ peening of Ti6Al4V was also conducted using treatment conditions AWJ A and AWJ B (Figure 8b). The apparent endurance strength of the untreated (control) Ti6Al4V defined at 1×10^7 cycles was 680 MPa. The endurance strengths of specimens treated with conditions AWJ A and AWJ B were 695 MPa and 724 MPa, respectively, and corresponded to an increase in fatigue strength of 3% and 6%, respectively.

DISCUSSION

A systematic study on the influence of treatment parameters on the surface texture and compressive residual stress resulting from AWJ peening of AISI 304 stainless steel was conducted. Kinetic energy of the garnet particles was transferred to the metal target and induced near-surface plastic deformation. A combination of plastic deformation and material removal resulted in an increase in surface roughness. Elastic recovery of the near-surface deformation resulted in development of compressive residual stresses. Undoubtedly, the kinetic energy and corresponding extent of plastic deformation are functions of the treatment parameters. The average surface roughness (R_a) resulting from AWJ peening of AISI 304 specimens ranged from approximately 5 to 14 μm. Results from the ANOVA indicated that jet pressure and abrasive size were the most influential parameters on the R_a and core roughness parameters (Figure 4). These results for AWJ peening are consistent with previous results for shot peening (28–30) and grit blasting (31, 32). Furthermore, despite the increase in surface

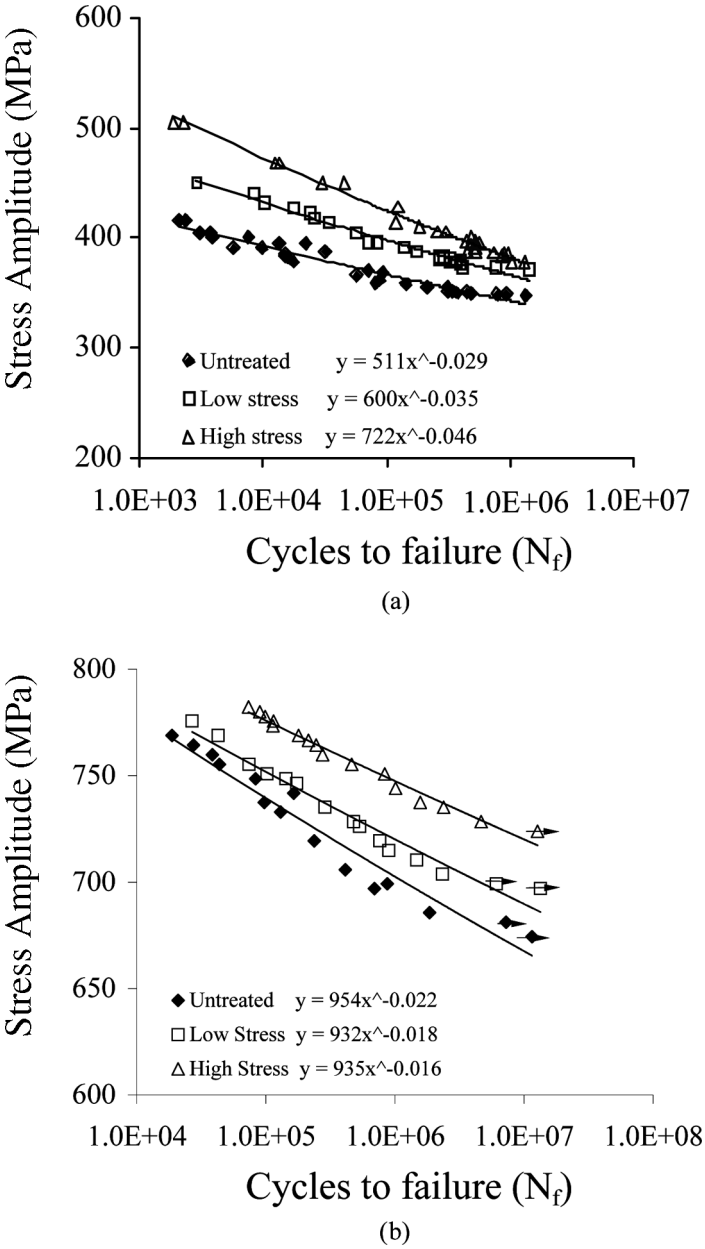

FIGURE 8 Stress life diagrams resulting from fully reversed fatigue loading of the AWJ peened and control (untreated) specimens. Arrows indicate specimens that did not fail. (a) AISI 304 stainless steel. (b) Ti6Al4V.

roughness, AWJ peening increased the fatigue strength of both the AISI 304 and Ti6Al4V. Nevertheless, the increase in fatigue strength of both metals was rather limited (<10%).

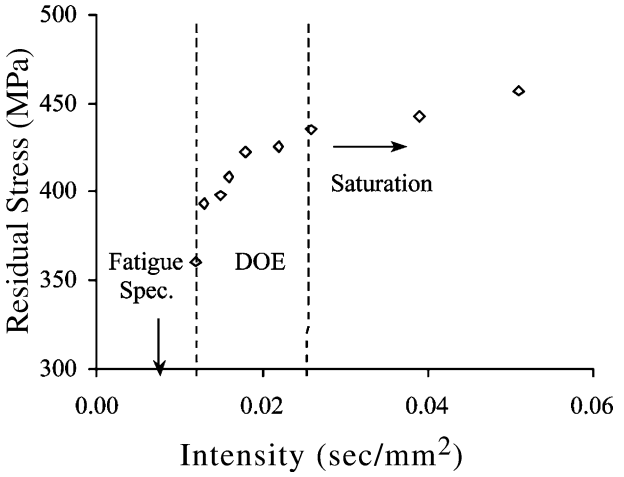

FIGURE 9 Change in residual stress with treatment intensity. The surface treatments were conducted using a jet pressure of 262 MPa, #54 mesh particles and standoff distance of 0.2 m. The saturation intensity was used in further treatments of the Ti6Al4V for maximizing the fatigue life (Figure 10).

Several studies have examined the influence of exposure time on residual stress and surface roughness resulting from surface treatments. For example Farrahi (33) reported that an increase in exposure time of shot peening increased the residual stress up to a threshold beyond which no further change occurred. An alternate description of exposure time could be achieved in terms of "treatment intensity," which is defined as the ratio of treatment time and surface area covered. Parametric conditions of the DOE resulted in a treatment intensity that ranged from 0.015 to 0.026 s/mm^2. As a result of rotation, treatment of the fatigue specimens occurred at an intensity of less than 0.01 s/mm^2. A separate study was performed using the optimum treatment conditions while also varying the treatment intensity (through traverse speed) from 0.01 to 0.05 s/mm^2. The residual stress increased consistently with treatment intensity until reaching "saturation" near 0.026 s/mm^2 (Figure 9). Further increases in intensity resulted in minimal changes in residual stress but facilitated material removal. Using the optimum treatment conditions and a traverse speed resulting in treatment intensity of 0.03 s/mm^2 a new set of Ti6Al4V specimens were treated and the corresponding fatigue strength distribution are compared with the control specimens in Figure 10. The apparent endurance strength increased to 845 MPa, nearly a 25% change. Thus, the fatigue strength resulting from AWJ peening of metals is sensitive to the treatment intensity. Though it is unknown if the threshold intensity identified in treatment of the AISI 304 is consistent with that in treatment of Ti6Al4V, the increase in endurance strength resulting from AWJ peening is consistent with that available from competing processes. For

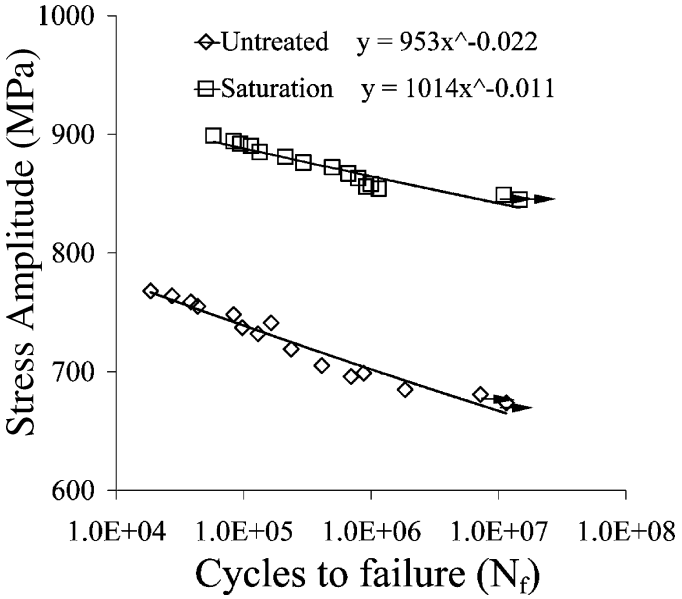

FIGURE 10 Stress life diagrams for the untreated (control) and AWJ peened Ti6Al4V. The AWJ peened samples were treated using an intensity of 0.025 s/mm^2, jet pressure of 262 MPa, #54 mesh particles and standoff distance of 0.2 m. Arrows indicate specimens that did not break.

example, Farrahi et al. (33) and Guilemany et al. (34) achieved an increase in endurance strength of steels through shot peening and grit blasting of between 10% and 20%.

Parametric trends identified in the present study are not consistent with those previously reported for AWJ peening (21) where a decrease in residual stress resulted from an increase in jet pressure and abrasive size in treatment of both Ti6Al4V and commercially pure titanium (CpTi). There it was rationalized that surface erosion of material occurring during the peening process resulted in stress relief. The difference in trends is likely to be attributed to the difference in methods used to measure residual stress in the two studies. Previous studies used X-ray diffraction where the residual stress was estimated from the average distribution over the depth of beam penetration (13 μm). The near-surface stress that resulted from the use of large abrasives and pressure could be partially released due to the large surface roughness and large relative surface irregularities with respect to the depth of beam penetration. Surfaces with smaller roughness would undergo much lower near-surface stress relief and likely to result in higher average residual stress over the depth of beam penetration. The simplistic approach used in estimating the residual stress in the present study did not provide information of the subsurface stress distribution resulting from AWJ peening. Therefore, it appears worthwhile

to evaluate the subsurface residual stress distribution resulting from AWJ peening in future studies.

According to the equivalent parametric trends for the residual stress and R_a, an increase in residual stress is not possible without a corresponding increase in surface roughness. Indeed, the relationship between the surface roughness and residual stress of the AWJ peened AISI 304 is shown in Figure 11. The contribution of surface roughness to crack initiation during cyclic loading has been a long-standing concern. Yet, the increase in near-surface dislocation density and development of macroscopic residual stress resulting from AWJ peening may be sufficient to retard crack initiation from surface irregularities. In an evaluation of the fracture surfaces using the SEM it was found that crack initiation in the untreated fatigue specimens occurred from the surface with radial lines extending from the origin of failure. In contrast fracture surfaces from the AWJ peened fatigue specimens showed that failure initiated approximately 150–200 μm below the treated surface. It appeared that the compressive residual stress suppressed crack initiation from the surface despite the large roughness resulting from AWJ peening. Kitsunai et al. (30) showed that crack initiation in shot peened specimens occurred at approximately 150–180 μm below the surface and in comparison to untreated specimens a 30% improvement in fatigue strength was achieved. Similarly, Tonshoff et al. (35) showed that WJ peening promoted a 30% improvement in fatigue

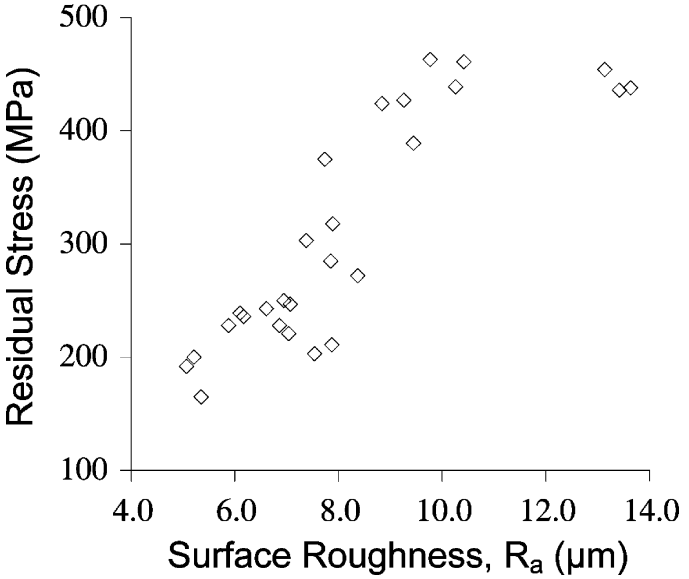

FIGURE 11 Relationship between the average surface roughness and residual stress resulting from AWJ peening of the AISI 304.

strength and that crack initiation commenced at a distance of 150–200 μm below the pended surface.

While AWJ peening can be used for simultaneous increase in surface roughness and development of a compressive residual stress, the process is also capable of changing the substrate's surface chemistry through impregnation of particles. Abrasive particles were found impregnated within the surface of fatigue specimens as shown in Figure 12. The abrasive particle concentration in the fatigue specimens estimated using the grid

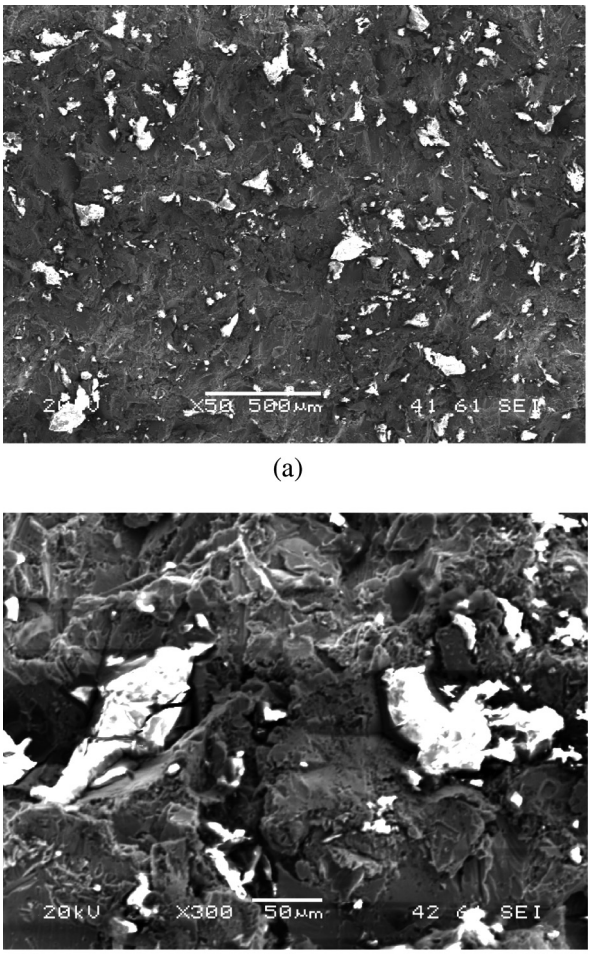

FIGURE 12 SEM micrographs of abrasive particles deposited on the surface of a fatigue specimen that resulted from AWJ peening. The treatment conditions consist of a jet pressure of 262 MPa, #54 mesh particles, traverse speed of 2.03 m/min and standoff distance of 0.2 m. (a) The surface of an AWJ peened specimen at 50X. (Note the impregnated particles.) (b) A magnified view of the surface from (a) at 300X.

method (23) was approximately 11%, which agrees with the results of previous investigations. Impregnated particles could be vital to bone on-growth in cementless fixation if they consist of the proper chemistry. However, the impregnated particles may act as stress concentration points on the surface of the material, and could be detrimental to the fatigue life. Nevertheless, the results of fatigue tests demonstrated that failure of the AWJ peened specimens initiated from a sub-surface location.

There are recognized limitations and sources of error that could contribute to variations in the experimental results. For example, the surface residual stresses in the AWJ peened AISI 304 were estimated from an approximation that is based on a linear distribution of stress from the neutral axis. The sub-surface distribution and differences in the depth of residual stress between treatments were not evaluated due to limitations of the simplistic approach. Future studies are planned using the layer removal method for determination of the distribution of residual stresses through thickness and a more precise estimate of the surface residual stress. Also, the conditions that resulted in the largest residual stress in treatment of the AISI 304 beams were used for treating the AISI 304 and Ti6Al4V fatigue specimens. Due to the axisymmetric specimen geometry and treatment, the magnitude of compressive residual stress in the fatigue specimens was not measured and may not be equivalent to that in the beams. While equivalent treatment intensity was used to maintain consistency in the treatments and residual stress, there were fundamental differences between the flat and cylindrical targets. According to the cylindrical shape of the fatigue specimens and effective jet treatment area, the angle of impingement was not limited to 90^{o}. Impingement on the periphery may have resulted in a lower residual stress than that possible from orthogonal impingement.

It is important to emphasize that residual stresses within the AWJ peened flat and cylindrical specimens were not assumed to be equivalent. Similarly, the residual stress resulting from treatment of the AISI 304 and Ti6Al4V fatigue specimens were not expected to be equivalent either. However, it was assumed that conditions resulting in the largest residual stress in the AWJ peened AISI 304 flat beams would also result in the largest residual stress in the fatigue specimens of both materials and that the parametric trends were the same. Due to the unique erosion resistance and constitutive behavior of the two metals that assumption may not be true. There are differences in the contributions of AWJ peening to the fatigue strength distributions of the AISI 304 (Figure 8a) and Ti6Al4V (Figure 8b) and this is expected to be partly attributed to self-heating effects on stainless steel under cyclic loading (36).

Despite these concerns and limitations, AWJ peening of both AISI 304 and Ti6Al4V fatigue specimens resulted in an increase in fatigue strength with respect to the untreated control. Thus, AWJ peening may serve as a

potent method for developing surfaces that require an increase in surface roughness and change in surface chemistry, while simultaneously maintaining or improving the fatigue strength.

CONCLUSIONS

An experimental investigation on the effects of AWJ peening on the residual stress, surface roughness and fatigue strength of selected orthopedic metals was conducted. A design of experiments (DOE) was implemented and the relative contributions of treatment effects on the dependent variables were obtained using an analysis of variance (ANOVA). The results obtained from this study showed that:

1. The average surface roughness (R_a) resulting from AWJ peening of the AISI 304 ranged from 5.08 μm to 13.64 μm. The surface texture resulting from AWJ peening was dependent on the treatment conditions and the R_a increased with increasing jet pressure and particle size.
2. Compressive residual stresses resulted from all AWJ peening conditions and the residual stress was primarily dependent on the particle size and jet pressure. The residual stress resulting from AWJ peening of AISI 304 ranged from 165 MPa to 463 MPa. The magnitude of residual stress increased with increasing particle size and jet pressure.
3. AWJ peening resulted in an increase in the fatigue strength of AISI 304 and Ti6Al4V. The fatigue strength increased the most with conditions that maximized the compressive residual stress despite the large increase in surface roughness. Using the optimum treatment conditions and the saturation intensity identified in treatment of AISI 304, the endurance strength of the Ti6Al4V was increased from 680 MPa to 875 MPa (25% increase).

REFERENCES

[1] Styles, C.M., Evans, S.L., and Gregson, P.J. (1998). Development of Fatigue Lifetime Predictive Test Methods for Hip Implants: Part I. Test Methodology. *Biomaterials*, 19(11–12):1057–1065.

[2] Sun, L., Berndt, C.C., Gross, K.A., and Kucuk, A. (2001). Material Fundamentals and Clinical Performance of Plasma-Sprayed Hydroxyapatite Coatings: A Review. *Journal of Biomedical Materials Research*, 58(5):570–592.

[3] Bourne, R.B., Rorabeck, C.H., Burkart, B.C., and Kirk, P.G. (1994). Ingrowth Surfaces. Plasma Spray Coating of Titanium Alloy Hip Replacements. *Clinical Orthopaedics and Related Research*, 298:37–46.

[4] Mauerhan, D.R., Mesa, J., Gregory, A.M., and Mokris, J.G. (1997). Integral Porous Femoral Stem. 5- to 8- Year Follow-Up Study. *Journal of Arthroplasty*, 12(3):250–255.

[5] Smith, S.E., Estok, D.M., and Harris, W.H. (1998). Average 12-Year Outcome of a Chrome-Cobalt, Beaded, Bony Ingrowth Acetabular Component. *Journal of Arthroplasty*, 13(1):50–60.

[6] Silverton, C.D., Roenberg, A.G., and Sheinkop, M.D. (1995). Revision total Hip Arthroplasty Using a Cementless Acetabular Component. *Clinical Orthopaedics and Related Research*, 319:201–208.

[7] Mallory, T.H., Head, W.C., Lombardi, A.V., Emerson, R.H., Eberle, R.W., and Mitchell, M.B. (1996). Clinical and Radiographic Outcome of a Cementless, Titanium, Plasma Spray-coated Total Hip Arthroplasty Femoral Component. Justification for Continuance of Use. *Journal of Arthroplasty*, 11(6):653–660.

[8] Martell, J.M., Pierson, R.H., Jacobs, J.J., Rosenberg, A.G., Maley, M., and Galante, J.O. (1993). Primary Total-Hip Reconstruction with a Titanium Fiber-Coated Prosthesis Inserted Without Cement. *Journal of Bone and Joint Surgery*, 75A(4):554–571.

[9] Cook, S.D., Georgette, F.S., Skinner, H.B., and Haddad, R.J. (1984). Fatigue Properties of Carbon- and Porous-Coated Ti-6Al-4V Alloy. *Journal of Biomedical Materials Research*, 18(5):497–512.

[10] Ducheyne, P., Martens, M., DeMeester, P., and Mulier, J.C. (1984). Titanium and Titanium Alloy Prostheses with Porous Fiber-Metal Coatings. In *Cementless Fixation of Hip Endoprostheses*, E. Morscher, ed., Springer-Verlag, New York, NY, 1983.

[11] Yue, S., Pilliar, R.M., and Weatherly, G.C. (1984). The Fatigue Strength of Porous-Coated Ti-6%Al-4%V Implant Alloy. *Journal of Biomedical Materials Research*, 18(9):1043–1058.

[12] Pilliar, R.M. (1987). Porous-Surfaced Metallic Implants for Orthopaedic Applications. *Journal of Biomedical Materials Research*, 21(A1):1–33.

[13] Cook, S.D., Thongpreda, N., Anderson, R.C., and Haddad, R.J. (1988). The Effect of Post-Sintering Heat Treatments on the Fatigue Properties of Porous Coated Ti-6Al-4V Alloy. *Journal of Biomedical Materials Research*, 22(4):287–302.

[14] Ranawat, C.S., Johanson, N.A., Rimnac, C.M., Wright, T.M., and Schwartz, R.E. (1986). Retrieval Analysis of Porous-Coated Components for Total Knee Arthroplasty. *Clinical Orthopaedics and Related Research*, 209:244–248.

[15] Morrey, B.F. and Chao, E.Y.S. (1988). Fracture of the Porous Coated Metal Tray of a Biologically Fixed Knee Prosthesis. *Clinical Orthopaedics and Related Research*, 228:182–189.

[16] Cofino, B., Fogarassy, P., Millet, P., and Lodini, A. (2004). Thermal Residual Stresses Near the Interface Between Plasma-Sprayed Hydroxyapatite Coating and Titanium Substrate: Finite Element Analysis and Synchrotron Radiation Measurements. *Journal of Biomedical Materials Research Part A*, 70(1):20–27.

[17] Tsui, Y.C., Doyle, C., Clyne, T.W. (1998). Plasma Sprayed Hydroxyapatite Coatings on Titanium Substrates. Part 1: Mechanical Properties and Residual Stress Levels. *Biomaterials*, 19(22):2015–2029.

[18] Yang, Y.C. and Chang, E. (2001). Influence of Residual Stress on Bonding Strength and Fracture of Plasma-Sprayed Hydroxyapatite Coatings on Ti-6Al-4V Substrate. *Biomaterials*, 22:1827–1836.

[19] Eberhardt, A.W., Kim, B.S., Rigney, E.D., Kutner, G.L., and Harte, C.R. (1995). Effects of Precoating Surface Treatments on Fatigue of Ti-6A1-4V. *Journal of Applied Biomaterials*, 6(3):171–174.

[20] Gil, F.J., Planell, J.A., and Padros, A. (2002). Fracture and Fatigue Behavior of Shot-Blasted Titanium Dental Implants. *Implant Dentistry*, 11(1):28–32.

[21] Arola, D., McCain, L., Kunaporn, S., and Ramulu, M. (2002). Waterjet and Abrasive Waterjet Treatment of Titanium: A Comparison of Surface Texture and Residual Stress. *Wear*, 249:943–950.

[22] Arola, D. and McCain, L. (2000). Abrasive Waterjet Peening: A New Method of Surface Preparation for Metal Orthopedic Implants. *Journal of Biomedical Materials Research. Applied Biomaterials*, 53:536–546.

[23] Arola, D. and Hall, C. (2004). Parametric Effects of Particle Deposition in Abrasive Waterjet Surface Treatments. *Journal of Machining Science and Technology*, 8:171–192.

[24] Wheeler, D. (1990). *Understanding Industrial Experimentation*. 2nd Ed., SPC Press, Inc., Knoxville, TN, 1989.

[25] Wheeler, D. (1989). *Tables of Screening Designs*, 2nd Ed., SPC Press, Inc., Knoxville, TN, 1990.

[26] Flavenot, J.F. (1996). Layer Removal Method. In *Handbook of Measurement of Residual Stresses*, J. Lu, ed., Fairmont Press, Inc., Lilburn, GA.

[27] Collins, J.A. *Failure of Materials in Mechanical Design: Analysis, Prediction, Prevention*, 2nd Ed. John Wiley and Sons, New York, NY, 1993.

[28] Wick, A., Holzapfel, H., Shulze, V., and Vohringer, O. (1999). "Effects of Shot Peening Parameters on the Surface Characteristics of Differently Heat Treated AISI 4140." Proceedings of the 7th International Conference on Shot Peening, Warsaw, Poland, pp. 42–53.

[29] Wagner, L. and Luetjering, G. (1996). "Influence of Shot Peening on the Fatigue Behavior of Titanium Alloys." Proceedings of the 1st International Conference on Shot Peening, Paris, France, pp. 453–460.

[30] Kitsunai, Y., Tanaka, M., and Yoshihisa, E. (1994). Effects of Shot Peening on Fatigue Strength of Ti6Al4V. *Journal of the Society of Material Science, Japan*, 43:666–671.

[31] Kaushik, N. and Sharma, S. (1982). "Effects of Some Operating Parameters in Direct Air Pressure Grit Blasting of Mild Steel Plate." Proceedings of the 10th All India Machine Tool Design and Research Conference, Durgapur, India, pp. 401–409.

[32] Mellali, M., Grimaud, A., Leger, C., Fauchais, P., and Lu, J. (1997). Alumina Grit Blasting Parameters for Surface Preparation in Plasma Spraying Operation. *Journal of Thermal Spray Technology*, 6:217–227.

[33] Farrahi, G., Lebrun, J., and Couratin, D. (1995). Effects of Shot Peening on Residual Stress and Fatigue Life of a Spring Steel. *Journal of Fatigue Fracture Engineering Material Structures*, 18:211–220.

[34] Guilemany, J., Llorca-Isern, N., and Szabo, J. (1996). Technical Note: Residual Stress Characterization of Grit Blasted Steel Surfaces. *Surface Engineering*, 12:77–79.

[35] Tonshoff, H., Kroos, F., and Marzenell, C. (1997). High Pressure Water Peening- a New Mechanical Surface-Strengthening Process. *Annals of the CIRP*, 46:113–116.

[36] Tian, H., Fielden, D., Brooks, C., Bruns, D., and Brotherton, M. (2001). Frequency Effects on Fatigue Behavior of Type 316 Stainless Steel: Experiment and Theoretical Modeling. D. Lesuer, Ed., Proceedings of the 2001 TMS Fall Meeting, Indianapolis, Indiana, November 4–8, 2001, pp. 161–174.